Appl. Phys. B 74, 419–425 (2002)
DOI: 10.1007/s003400200825

Applied Physics B
Lasers and Optics

A. HEISTERKAMP[1,✉]
T. RIPKEN[1]
T. MAMOM[2]
W. DROMMER[2]
H. WELLING[1]
W. ERTMER[3]
H. LUBATSCHOWSKI[1]

Nonlinear side effects of fs pulses inside corneal tissue during photodisruption

[1] Laser Zentrum Hannover e.V., Hollerithallee 8, 30419 Hannover, Germany
[2] Institut für Pathologie, Tierärztliche Hochschule Hannover, Bünteweg 17, 30559 Hannover, Germany
[3] Institut für Quantenoptik, Universität Hannover, Welfengarten 1, 30167 Hannover, Germany

Received: 12 October 2001 / Revised version: 13 February 2002
Published online: 14 March 2002 •

ABSTRACT In order to evaluate the potential for refractive surgery, fs laser pulses of 150-fs pulse duration were used to process corneal tissue of dead and living animal eyes. By focusing the laser radiation down to spot sizes of several microns, very precise cuts could be achieved inside the treated cornea, accompanied with minimum collateral damage to the tissue by thermal or mechanical effects. During histo-pathological analysis by light and transmission electron microscopy considerable side effects of fs photodisruption were found. Due to the high intensities at the focal region several nonlinear effects occurred. Self-focusing, photodissociation, UV-light production were observed, leading to streak formation inside the cornea.

PACS 42.62.Be; 42.65Re; 87.80.Rb

1 Introduction

The application of fs laser pulses in medicine is a growing field of interest, for example, in refractive surgery for vision correction [1–3], neurosurgery [4] or nanosurgery in single cells [5]. The main advantage of the use of fs pulses is the high cutting precision in the μm range accompanied by minimal collateral damage. Focusing of the ultrashort laser pulses leads to very high field intensities in the focal region. Due to these high intensities, free electrons are generated and accelerated by nonlinear absorption processes [6], resulting in an optical breakdown inside the medium. In medical applications this breakdown is used to achieve a cutting effect inside biological tissue, this process is known as photodisruption. Thus, it is possible to manipulate tissue, even inside the bulk of the material, by focusing the radiation below the surface. In contrast to what is known from application of ns pulses in ophthalmology during the treatment of secondary cataract by Nd : YAG laser capsulotomy, the mechanical and thermal damage in the surrounding tissue is reduced dramatically [4, 7].

Because of the short pulse duration of some hundred fs, the threshold of approximately 10^{11} W cm^{-2} for creating a plasma can be reached at energies in the range of 1 μJ or even below, when focusing the laser radiation to spot sizes of several microns. In the case of aqueous media a cavitation bubble accompanied by a shock wave develops at the breakdown region, due to the explosive heating of the fluid. In biological tissue possible acoustical damage due to these phenomena might occur. Typically, these effects scale with the energy of the laser pulse and are, therefore, reduced during application of fs laser pulses.

In the field of refractive surgery, ultrashort laser pulses can be used for vision correction. To produce a refractive effect, a so-called lenticule has to be prepared within the cornea of the treated eye. Thereafter, a cut from the lenticule towards the surface of the cornea is created, allowing the eye to be opened and the lenticule to be extracted. The process is shown in Fig. 1.

The lack of the extracted tissue leads to an altered surface curvature of the eye and, thus, to a change in its refractive power. The shape of the lenticule corresponds to the desired change in refractive power. Although the mechanical and thermal side effects have already been shown to be small, several other side effects may occur, due to the nonlinear character of photodisruption.

In this paper, these additional effects, such as self-focusing [8], photodissociation by multiphoton absorption and generation of higher harmonics, are further investigated. Therefore, several samples of enucleated pig eyes were subjected to the surgery procedure, followed by histopathological analysis, using light and electron microscopy. To

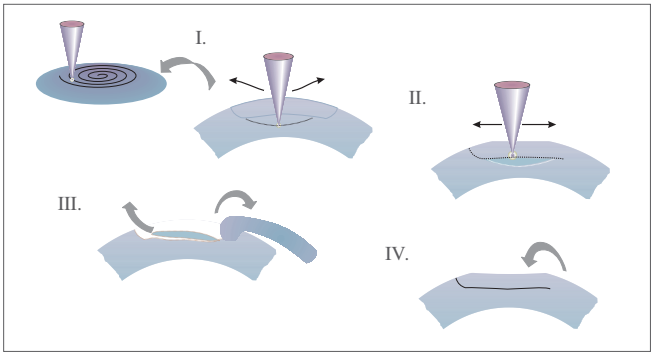

FIGURE 1 Principle of the fs-LASIK procedure. A flap and a lenticule is created inside the cornea by focusing of the laser radiation and scanning of the laser focus in a spiral pattern (I–II). Afterwards, the flap is opened and the lenticule is extracted by the surgeon (III–IV)

✉ Fax: +49-511/2788-100; E-mail: ah@lzh.de

study long-term effects, in vivo studies with 2 living rabbits were performed. Additionally, generation of higher harmonics in ex vivo eyes was studied by an optical multichannel analyser. The gaseous compounds produced inside the cornea during the cutting were analysed in a combined gas-chromatograph/mass-spectrometer setup.

2 Experimental methods

2.1 *Laser system*

The laser system used in this study consisted of a titanium : sapphire amplifier, seeded by a mode-locked erbium fiber laser oscillator. The pulses from the Er^{3+} oscillator, at a repetition rate of 66 MHz, were frequency-doubled in a chirped, periodically poled, lithium-niobate crystal, resulting in 2-mW output power at a central wavelength of 780 nm. Subsequently, these pulses were amplified by means of chirped pulse amplification (CPA) [9] in a titanium : sapphire regenerative amplifier pumped by a frequency-doubled Nd : YLF laser. The system allowed variable repetition rates of up to 3 kHz at output powers of 300 mW. The minimum achievable pulse duration of the system was approximately 150 fs. Longer pulse durations were achieved by detuning the compressor system and not fully recompressing the output pulse, leading to a defined chirp and, thus, a longer pulse duration.

During all experiments the pulse duration was controlled by a single-shot autocorrelator. The energy was adjusted by a variable attenuator or with the help of a half-wave plate in front of the compressor system, leading to the attenuation of the uncompressed pulses at the grating of the compressor setup.

2.2 *Intrastromal cuts*

In order to perform intrastromal cuts and incisions, a computer-controlled, two-axis scanner system guided the amplified pulses via an f-Theta optic towards the treated eyes (see Fig. 2).

The focusing optic had a focal length of 75 mm, leading to a spot size of approximately 5 μm. To keep the treated eyes in a fixed position, a suction unit was integrated into the focusing system. This suction unit contained a glass plate, which flattened the cornea over a working field of 10-mm diameter. At the edges of the glass plate, gentle suction was applied to keep the eye in position. The whole suction ring was mounted on a microtranslation stage, which allowed variation of the z-position of the unit to the f-Theta optic with sub-micron resolution. Combined with the two scanning mirrors, 3D translation of the laser focus within 9 mm depth and over a working field of 10-mm diameter was possible.

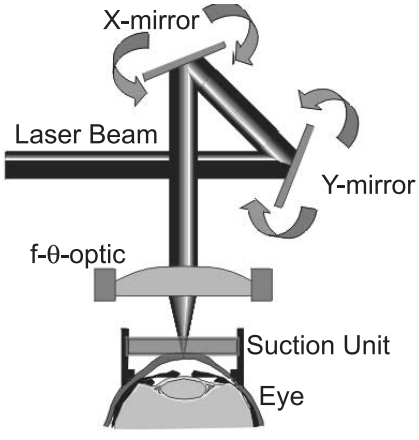

FIGURE 2 fs-LASIK setup. The laser radiation is delivered over a scanning and focusing unit. The eye is held fixed by a suction unit

Ex vivo experiments were performed on freshly enucleated pig eyes within several hours after enucleation. Following the laser treatment, the eyes were fixed in glutarate dealdehyde (3.5%) and afterwards prepared for histological sections (1.4-μm thickness) in glycidyl methacrylate–methylmethacrylate (GMA/MMA) or critical-point dried and analysed by scanning electron microscopy (SEM) or transmission electron microscopy (TEM), respectively.

The in vivo experiments were conducted with 2 living, female New Zealand white rabbits at an age of 24 and 30 months. From each animal, one eye was subjected to surgery and one was kept untreated. To study wound healing and long-term effects, the post-op follow-up was chosen to be 7 and 14 days. During the surgery the animals were kept under general anaesthesia. After the follow-up, the animals were sacrificed and the eyes were prepared for histopathological analysis.

The animals used in this study were treated under German animal welfare regulations.

2.3 *Higher harmonic generation*

To determine possible wavelength conversions in the focal region during the surgery procedure, experiments using an optical multichannel analyser were performed, the setup is shown in Fig. 3.

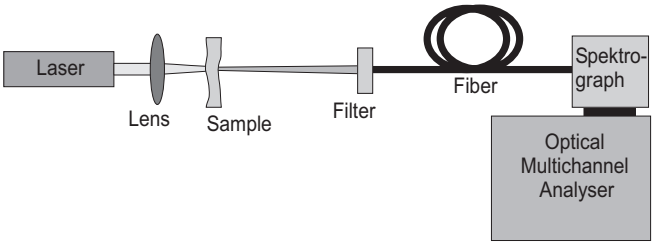

FIGURE 3 Setup of the higher harmonic generation

During measurement, a sample of freshly enucleated pig cornea was placed in the focal region; it was mounted between two thin glass plates made out of fused silica. The residual laser radiation was blocked behind the sample by a dichroitic filter, ranging from 700 nm down to 200 nm. The residual light behind the filter was coupled into a fiber, which delivered the light to the optical multichannel analyser. The signals were corrected for the absorption of the glass plates, fiber transmittance and detector sensitivity.

2.4 *Chemical analysis*

To observe possible chemical processes taking place during photodisruption, the gaseous constituents pro-

duced in the focus region were collected and subjected to gas chromatography. Therefore, a sample of pig cornea was sealed in an airtight vessel with a volume of 1.5 ml. To reduce disturbance from the background air, the vessels were filled with argon. The gas chromatograph consisted of a 0.53-mm-diameter capillary column and an integrated molecular sieve with 5-Å-diameter pores. The gaseous constituents were detected after they had diffused through the column using a thermal conductivity detector. Since larger fragments diffuse at a slower rate, each constituent causes a distinct signal in time. By measuring this specific time, the simple gaseous constituents of a gas sample, such as hydrogen or nitrogen, can be identified, by comparison with the signals measured from pure samples injected into the apparatus. To be able to determine even larger and complex molecules, a mass spectrometer was coupled to the columns of the gas chromatograph.

The laser radiation was focused through the wall of the glass vessel onto the cornea sample to generate gases by photodisruption. In order to achieve accelerated gas production, the highest possible energy, approximately 300 μJ, was applied. Nevertheless, the results obtained at such high energies are still comparable to low-energy regimes, because the energy density at the focal region remains nearly constant for different pulse energies when fs pulses are applied. This is mainly because no heating of the created plasma occurs, due to the very short pulse duration [6].

Directly after application of several laser pulses, a part of the gas in the vessels was extracted and injected into the gas chromatograph. Additionally, a second sample containing a cornea was used as a blind sample, to which no laser pulses were applied.

3 Results

3.1 *Intrastromal cuts*

Figure 4 shows an SEM graph of a treated porcine eye in which a lenticule of 80-μm thickness and 3-mm diameter was prepared. The applied laser energy was 1 μJ at a pulse duration of 160 fs and a spot size of 5 μm. The spot separation, with which each pulse was placed beneath the previous pulse, was chosen to be 6 μm. The flap was opened directly after treatment and the lenticule only partly extracted to be preserved for histopathological analysis. The thickness of the corneal flap was 120 μm, with a diameter of 4 mm. The detail of Fig. 4 shows the corneal bed of the flap in higher magnification. The interface of the created cut is very smooth and comparable to results obtained with a mechanical keratom.

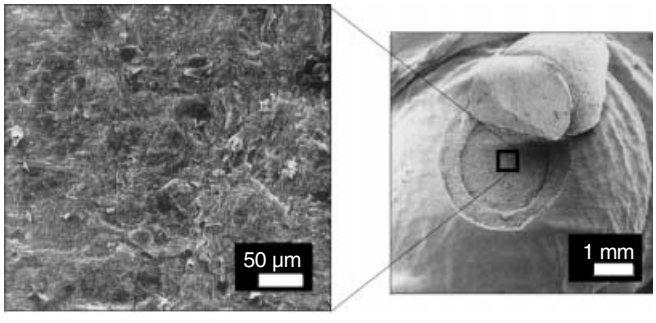

FIGURE 4 SEM graph of a porcine eye globe with a flap and lenticule prepared by the fs laser

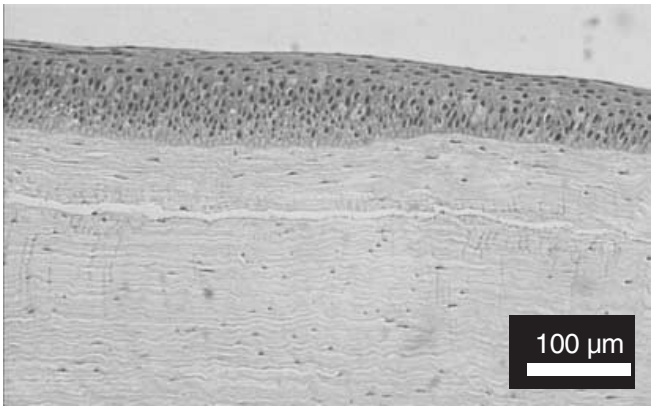

FIGURE 5 Histological section of a porcine eye globe showing a subsurface cut at 120-μm depth

The minimum mechanical and thermal side effects are visualized by histopathological anaylsis. In Fig. 5 the histological section of a porcine eye globe treated with identical parameters can be seen. The laser cut is visible about 120 μm below the surface of the eye. The cut offers a precision in the μm range, showing no big bubbles or remaining tissue bridges, as found in earlier experiments [10]. Any thermal damage would appear in a darker colour due to HE-staining and was absent in all histological sections. The thermal effects are therefore determined to be in or even below the μm range, i.e. the resolution of the light microscope. The layers in front of and behind the focal region remain unaltered.

Even in living tissue the side effects could be determined to be very small. In both animals a flap of 3 mm in diameter was prepared, opened and repositioned. Within several hours after the treatment, the treated corneae were already clear and showed only a slight central subepithelial haze, which disappeared within 24 h after the surgery, as proven by slit-lamp observation. The epithelium remained intact 24 h after treatment too. The edges of the cut were still visible even 14 days after the treatment, but showed no strong wound-healing reaction in terms of fibroblast migration. The surface of the cornea was quite smooth, and no excessive wound-healing reaction involving collagen reproduction could be noticed.

3.2 *Streak formation*

During histological analysis of the treated eyes, additional side effects were observed. Very small streaks originating in the focal plane and reaching up to 100 μm towards the endothelium and epithelium in both directions. These streaks are near the resolution limit of the light microscope, having diameters of less than a micron.

Moreover, the in vivo studies showed that even several days after the treatment the streaks were still noticeable (see Fig. 6). In front of and behind the cut, these streaks run vertical to the cut, at a distance of 6 μm, corresponding to the spot seperation of the applied laser pulses. Obviously, a wound-healing reaction due to these streaks was not noticeable, although the tissue alteration in the streaks seems to be permanent, as the streaks were found up to 14 days after treatment.

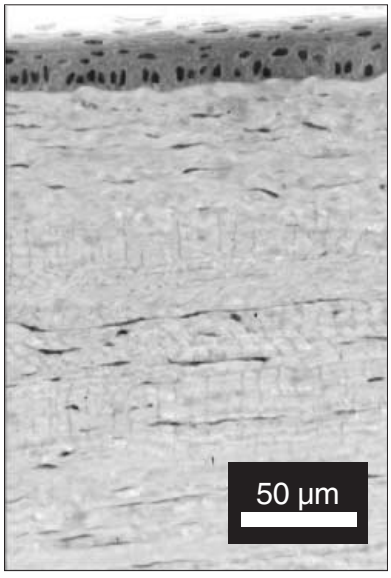

FIGURE 6 Histological cut of a streak formation in a rabbit eye 7 days after treatment. The cut can be seen by proliferated keratocytes 150 µm below the surface; perpendicular to the cut, streaks at a distance of 6 µm are observable

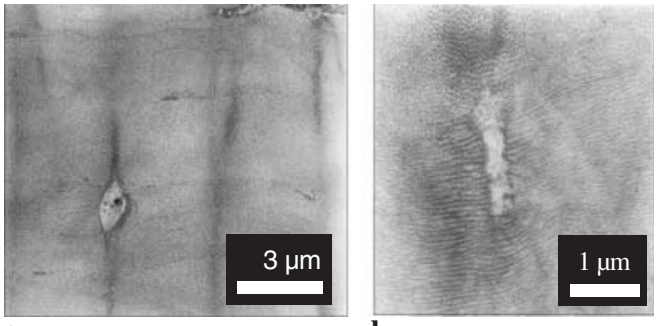

FIGURE 7 TEM graph of intrastromal streaks in a porcine eye globe. **a** 3150× magnification, **b** 20000× magnification. The streaks are running vertical through the picture, appearing as a darker staining of the fibrils

TEM graphs of the histologies of the ex vivo eyes were made in order to determine the nature of these streaks.

Figure 7a shows three streaks inside the cornea of a porcine eye globe. The extent of a single streak can be determined to be 300–500 nm, which is below the diffraction limit of the focused laser beam.

In Fig. 7b another streak at a higher magnification is shown. In the center of the streak, a breakdown can be seen, showing disrupted collagen fibrils in a zone of 350-nm diameter. In front of and behind this micro-cavity, the structures of the single fibrils are left intact, but appear with a darker staining. Nearly no melting in fibrils due to heating effects was observed. Only at the rim of the disrupted fibrils was a small heat-affected zone visible, with a diameter of less than 150 nm.

3.3 *Third harmonic generation*

By focusing the ultrashort laser pulses into a corneal sample, UV-light production at a wavelength of 260 nm was found. The spectra received by the optical multichannel analyser is shown in Fig. 8. At 780 nm the strong peak of

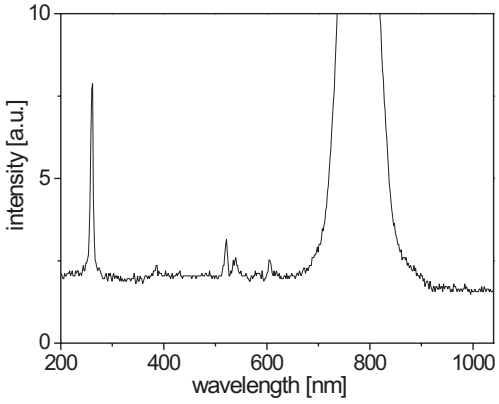

FIGURE 8 Spectra measured by the optical multichannel analyser behind the corneal sample

the residual laser radiation can be seen, which still passes through the filter. A second peak at 260 nm is visible. The small peaks at 500–600 nm are due to scattered background light.

With respect to the losses in the filter and the fiber delivering the light to the analyser, and the different sensitivity of the detector at the two wavelengths, the conversion efficiency was found to be 2.5×10^{-5}. During the experiments the peak at 260 nm was only visible when the laser focus was placed in the posterior part of the sample, i.e. close to the endothelium of the cornea, near the silica glass plate. If the laser focus was moved into the silica plate, the peak vanished instantly. The same happened when the laser focus was moved deeper into the corneal sample. In addition, no UV-light was detected at the boundary of the silica glass and air.

3.4 *Chemical analysis*

In all treated corneal samples fractions of molecular hydrogen were found. As already shown by the authors in previous experiments [11], photodissociation of water molecules was observed. In contrast to the results found previously in pure water, additional gas constituents were produced in the corneal sample due to the bond-breaking of biological molecules.

Figure 9 shows the results of the gas chromatography. Due to the very high diffusivity of hydrogen, the hydrogen molecules pass the capillary column of the apparatus very quickly and appear at the thermal conductivity detector approximately 2.5 min after injection of the sample. The second peak at $t = 4.5$ min is due to oxygen. The third peak was found to be residual nitrogen, which did not originate from the laser treatment, as it was found in the blind sample. A certain amount of oxygen was found in the blind sample too. In contrast, two more peaks were found only in the treated samples, at $t = 11$ and 35.5 min. With the help of the mass spectrometer, it was possible to detect the mass spectra of the single peaks. The mass spectra of the peak at a rise time of 35.5 min is plotted in Fig. 10, showing the mass–charge ratio versus the relative incidence.

The main constituents of the gas peak have a mass–charge ratio of 28, followed by some constituents at 12, 16 and 18. According to the NIST Library, carbon monox-

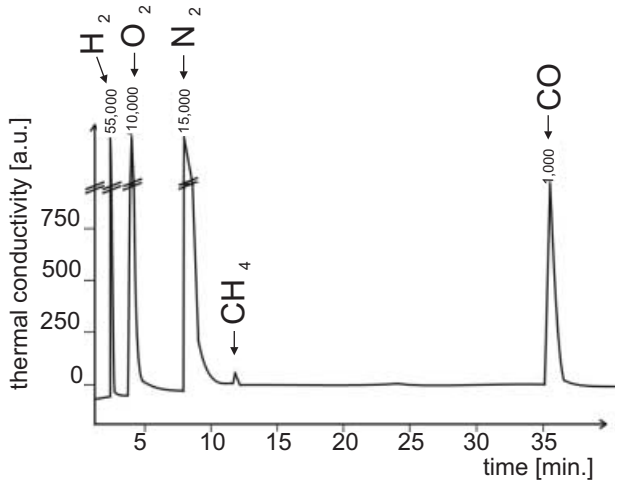

FIGURE 9 Results of gas chromatography showing peaks at 2.5, 4.5, 9, 11 and 35.5 min rise time

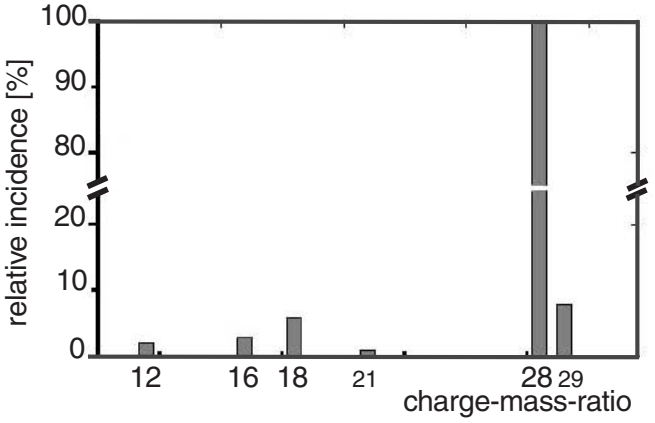

FIGURE 10 Results obtained with the mass spectrometer, showing mass spectra of the measured peak at $t = 35.5$ min

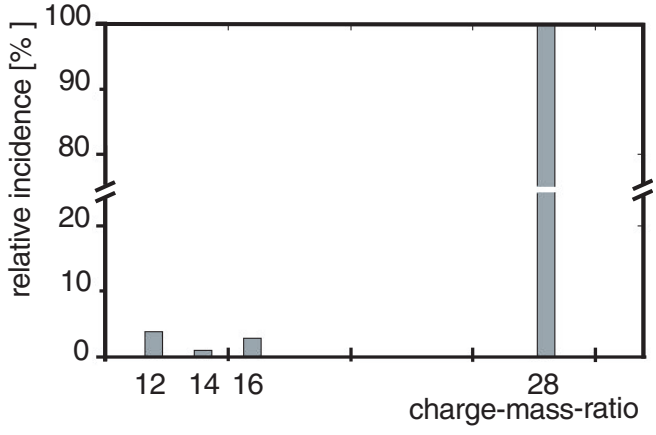

FIGURE 11 Mass spectra of CO as given by the NIST library

ide has the mass spectra shown in Fig. 11. Therefore, the gas peak at 35.5 min was determined to be CO. The small deviations are due to the small amount of CO gas in the sample. Analogously, the peak at 11 min was determined to be methane, CH_4, together with some fragments of CH_3 and CH_2.

4 Discussion

The results of the ex vivo experiments show the potential of fs laser pulses to perform intrastromal cuts and to create so-called lenticules. The procedure of opening the flap and extracting the lenticule proved to be extremely easy, even in living animals. The stromal cuts showed little surface roughness, comparable to that of conventional, mechanical keratom cuts. During the experiments a strong dependence on the pulse energy and spot size of the laser used was found. Therefore, the use of a minimum of energy, on the order of 1 μJ or even below, and small spot sizes, of 5 μm, is desirable. With a reduction in the spot size and the use of larger focusing apertures, the required energy to achieve a breakdown would be reduced. This reduction results in smaller side effects, such as cavitation and bubble formation, enabling a higher cutting precision. The width of the intrastromal cut was determined by histological analysis to be in the range of 2–3 μm. Even smaller spot sizes would lead to pulse energies in the nJ regime; however, the surgery time would increase to values of above 10–20 min, because of the very small width of the cut.

The fs laser offers another advantage when compared to the mechanical keratome: the edges of the flap can be made much steeper, offering better support to the repositioned flap, thus keeping it in a more defined position. As a further result of the histologies nearly no visible thermal damage of the tissue could be detected by light microscopy. With the help of TEM graphs, this damage was determined to be in the range of 150 nm. The wound healing after treatment was found to be nearly identical with what is known from LASIK surgery [12]. Only mild scarring at the edge of the flap could be noticed, as there is no entry point of the blade like during the use of the keratom, which leads to stronger wound-healing reactions.

As a new side effect of fs photodisruption, the generation of intrastromal streaks was noticed. These streaks reached up to 100 μm in length, with diameters in the range of 300–500 nm. Since the diameter is below the diffraction limit of the laser beam, these streaks are evidence that self-focusing occurs. As is given in theoretical works [13], collapse of the beam occurs in front of the focal plane, leading to very high field intensities that alter the tissue structure in these streaks. In the focal plane, the intensity reaches the breakdown threshold, leading to a well-defined cutting plane. Behind the focal plane the beam is still under the influence of self-focusing, again leading to streak formation. As was proven in the in vivo experiments, this tissue alteration is still visible 7 and 14 days after treatment and, thus, seems to be permanent. The TEM graphs of these streaks show the intact structure of the single collagen fibrils, a change in vision quality, such as corneal haze, could not be noticed. However, the vision quality was only determined by slit-lamp observation of the treated corneae in terms of corneal clearness. Although the vertical streaks have no visible refractive effect, their origin remains unclear. Unless a full understanding of the underlying mechanism and tissue alterations is achieved, it will be highly desirable to completely avoid them.

Several physical processes may be considered to be the origin of these streaks: First, the very high free-electron densities of up to 10^{18} cm^{-3} might cause chemical alteration of the single fibrils. Second, these electrons might lead to a temperature rise and, thus, to thermal alteration of the tissue, although such a thermal influence seems unlikely with respect to the histological findings. Third, the very high field intensities near the focal region can cause effects like electro-striction, which leads to mechanical compression of the fibrils and, thus, mechanical damage. In any case, the production of the streaks is based on the occurrence of self-focusing. To suppress self-focusing, higher apertures should be employed. In initial experiments with a higher aperture (NA $>$ 0.2), streak formation was significantly reduced.

As shown in this study, third harmonic generation at the boundary of the corneal tissue is very strong, with efficiencies of up to 10^{-5}. Due to the symmetry conditions inside the cornea, the generation of second harmonic radiation is suppressed and only third harmonic is possible in principle. However, this radiation can only be generated efficiently if a positive wave-vector mismatch between the fundamental and the harmonic beam is given [14]. In the case of an interface, as considered by Tsang [15], phase matching and efficient third harmonic generation is achieved by breaking the symmetry conditions in the focal region. Therefore, the production of 260-nm radiation is most likely during the last part of the surgery procedure, in which the laser is focused near the upper surface of the eye. Corresponding damage at the cellular level of the epithelium and on single fibrils could not be found by histopathological analysis.

Moreover, photodissociation happens in the focal region, as gases such as H_2, CO and CH_4 were found. Therefore, the high laser intensity not only causes disruption and evaporation of the tissue, but actually breaks the molecular bonds. Other fragments of biological molecules, such as free radicals, should also be produced, but they were not detectable with the setup used. These radicals might lead to cell damage or death at the focal point; they can thus induce tissue alteration effects over a longer time scale after exposure, as reported by Toth et al. [16], who found visible retinal lesions 24 h after fs laser pulse exposure which were not observable directly after treatment.

5 Conclusion

Side effects of fs photodisruption are small in terms of mechanical or thermal damage to the surrounding tissue. However, while reducing these side effects with shorter pulse durations, one has to deal with several nonlinear effects induced by the higher field intensities of the laser pulses.

As proven by ex vivo and in vivo experiments, refractive surgery using a fs laser is feasible, as shown by other groups [1, 3]. The surface quality of the cuts prepared inside corneal samples is comparable to or better than what is known from mechanical knifes or microkeratomes. However, the cutting quality strongly depends on the parameters used, such as pulse energy, pulse duration, spot size and focusing optics, as already shown by the authors [17].

Additionally, several nonlinear effects can be observed during application of ultrashort laser pulses. Self-focusing leads to tissue alteration on a nm scale, which is still visible 2 weeks after treatment. The nature of this alteration is not quite clear yet, and it should be evaluated in the near future. As possible reasons for this tissue alteration, high field intensities or the high free electron densities are thinkable. Further studies using immunohistology to determine the type of alteration of the corneal fibrils are underway.

Furthermore, third harmonic generation leads to 260-nm radiation at the boundaries of the corneal stroma and might alter the upper tissue layers too. However, no corresponding damage could be found. Nevertheless, the possible influence of third harmonic generation should be controlled during long-term studies. Work by Rockwell et al. has already proposed the possibility of tissue damage induced by continuum generation [18], although continuum radiation is only observed at relatively low numerical apertures (NA $<$ 0.2) and can thus be suppressed by using higher numerical apertures.

As another nonlinear effect, photodissociation was found to occur, probably induced by multiphoton absorption at the breakdown region. However, this effect was measured at very high pulse energies. The amount of gases produced at energies of some μJ is quite small and should therefore have no impact on the surgical outcome. In summary, refractive surgery by ultrashort laser pulses is possible, offering very high precision and leading to only small mechanical and thermal side effects. However, this cutting process is accompanied by several new nonlinear effects, which may have low impact on the surgical outcome, but may be helpful in a more thorough understanding of the mechanisms of fs breakdown in tissue.

ACKNOWLEDGEMENTS The authors would like to thank Mr. Stefan Barcikowski for his help in performing the chemical analysis. This work has been supported by the German Research Foundation (DFG), project no. Lu498/1, and the German Ministry of Education and Research (BMBF), project no. 13N7793.

REFERENCES

1 X. Liu, R.M. Kurtz, A. Braun, H.H. Liu, Z. Sacks, T. Juhasz: CLEO: Conf. Lasers Electroopt. (OSA Tech. Digest Ser. 169) **11**, 169 (1997)
2 W. Kautek, S. Mitterer, J. Krüger, W. Husinsky, G. Grabner: Appl. Phys. A **58**, 513–518 (1994)
3 T. Juhasz, F.H. Loesel, R. Kurtz, C. Horvath, J.F. Bille, G. Mourou: IEEE J. Sel. Top. Quantum Electron. **5**(4), 902 (1999)
4 F.H. Loesel, J.P. Fischer, M.H. Götz, C. Horvath, T. Juhasz, J. Noack, Suhm, J.F. Bille: Appl. Phys. B **66**, 121 (1998)
5 K. König, I. Riemann, W. Fritzsche: Opt. Lett. **26**(11), 819 (2001)
6 A. Vogel, J. Noack, D. Theisen, S. Busch, U. Parlitz, D.X. Hammer, G.D. Noojin, B.A. Rockwell, R. Birngbruber: Appl. Phys. B **68**, 271 (1999)
7 D. Stern, R.W. Schoenlein, C.A. Puliafito, E.T. Dobi, R. Birngruber, J.G. Fujimoto: Arch. Ophthalmol. **107**, 587 (1989)
8 J.H. Marburger: Prog. Quantum Electron. **4**, 35 (1975)
9 G. Mourou: Appl. Phys. B **65**, 205 (1997)
10 H. Lubatschowski, G. Maatz, M. Rudolf, A. Heisterkamp, U. Hetzel, W. Drommer, H. Welling, W. Ertmer: Graefe Arch. Exp. Clin. Ophthalmol. **238**, 33 (2000)

11 G. Maatz, A. Heisterkamp, H. Lubatschowski, S. Barcikowski, C. Fallnich, H. Welling, W. Ertmer: J. Opt. A: Pure Appl. Opt. **2**, 59 (2000)
12 J. Wachtlin, K. Langenbeck, S. Schründer, E.P. Zhang, F. Hoffmann: J. Refract. Surg. **15**, 451 (1999)
13 Q. Feng, V. Moloney, E.M. Newell, E.M. Wright, K. Cook, P.K. Kennedy, D.X. Hammer, A. Rockwell, C.R. Thompson: IEEE J. Quantum Electron. **QE-32**(2), 127 (1997)
14 R.W. Boyd: *Nonlinear Optics* (Academic Press, Boston 1992)
15 T.Y.F. Tsang: Phys. Rev. A **52**(5), 4116 (1995)
16 C.A. Toth, D.G. Narayan, C.P. Cain, G.D. Noojin, K.P. Winter, B.A. Rockwell, W.P. Roach: Invest. Ophthalmol. Visual Sci. **38**(11), 2204–2213 (1997)
17 A. Heisterkamp, T. Ripken, E. Luetkefels, W. Drommer, H. Lubatschowski, H. Welling, W. Ertmer: Proc. SPIE **4161**, 52 (2000)
18 B.A. Rockwell, D.X. Hammer, R.A. Hopkins, D.J. Payne, C.A. Toth, W.P. Roach, J.J. Druessel, P.K. Kennedy, R.E. Amnotte, B. Eilert, S. Phillips, G.D. Noojin, D.J. Stolarski, C. Cain: J. Laser Appl. **11**(1), 42 (1999)